10 % loss of incident power through solar reactor window: myth or good rule of thumb?

Victor Pozzobon[1] ✉

[1]Université de Toulouse, centre RAPSODEE, UMR CNRS 5302, Mines Albi, Campus Jarlard, route de Teillet, 81013 CT Albi Cédex 09, France

It is of common knowledge in the field of solar reactor design that a beam crossing a window losses 10 % of its incident power. Yet, this affirmation is not supported by many published scientific evidences. In this work, a heat flux mapping method was used to determine the heat flux distributions at the focal spot of a solar concentrating device without and with a window on the incident beams' trajectory. The presence of a window on the beams' trajectory induces a 12 % loss of the total power and a 11 % decrease of the peak heat flux density.

Correspondence: ***victor.pozzobon@mines-albi.fr***

1. Introduction

Concentrated solar power can be used to supply heat at high temperature. It features several advantages compared to conventional fossil fuel burning methods. Among them is the fact that concentrated solar power supplies clean heat, i.e., without combustion fumes. Indeed, those fumes may alter or even destroy the heated material, e.g. decomposition of limestone (1). In addition, whenever the reacting atmosphere needs to be controlled, it is common to add a windowed aperture to the reactor design (2–4). This window ensures the airtightness of the reactor while allowing the solar heat flux to enter it.

Nevertheless, adding a window comes with one main drawback: it lowers the amount of energy entering the reactor. Indeed, the incident flux crosses the window and therefore loses part of its power because of in medium absorption and dioptres reflections. It is, most of the time, quoted as common knowledge in the field of solar reactor design that crossing a window induces a 10 % loss of the incident power. Yet, only one research paper was found to support this claim, in the very particular case of a dome (5), and not of a flat window. Furthermore, this claim is not complete for it only regards the total power: it does not precise whether or not the heat flux distribution is modified.

In order to assess for the validity of this claim, the heat flux distributions at the focal spot of a solar concentrating system were mapped with and without a quartz window on the beams' trajectory. Then, the total incident power and the shape of the heat flux distribution were compared.

2. Materials and Methods

Figure 1 shows a schematic of the solar concentrating device, i.e. an artificial sun, and the heat flux measurement material. To map the incident heat flux, a screen is set in front of the artificial sun at the focal spot. Thus, the beams coming out of it are intercepted by the screen. As beams' energy is absorbed by the screen, its temperature rises. The temperature variations are recorded by IR camera. Then using inverse methods the temperature elevation is used to compute the incident heat flux distribution over the screen. A 2D model is used to link temperature (T) rise with incident heat flux (Ψ). It accounts for the contribution of the incident radiative heat flux as well as convective and radiative heat losses (Eq. 1).

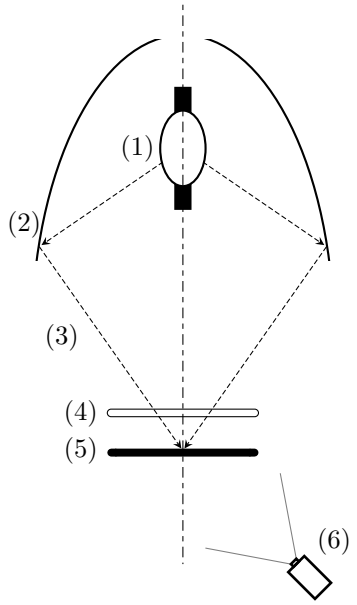

Fig. 1. Experimental apparatus schematics (6). (1) - 4 kW xenon arc lamp, (2) - elliptical mirror, (3) - a ray, (4) - removable quartz window, (5) - screen, (6) - camera

$$\rho c_p \frac{\partial T}{\partial t} = \lambda \Delta T + \frac{\alpha_p \phi}{e} - \frac{2h}{e}(T - T_{sur}) - \frac{(\epsilon_p + \epsilon_s)\sigma}{e}(T^4 - T_{sur}^4) \quad \textbf{(1)}$$

With ρ, c_p, λ, α, ϵ, e screen density, heat capacity, conductivity, absorptivity, emissivity and thickness respectively, T_{sur} and h, surrounding temperature and convective heat flux coefficient.

The model is solved for each pixel of the recorded images using ordinary least square method. Once completed, this procedure yields a map of the incident heat flux. The solar concentrating system and the heat flux mapping method used in this work have been extensively described in (6).

A 3 mm thick flat quartz sheet was used to simulate a re-

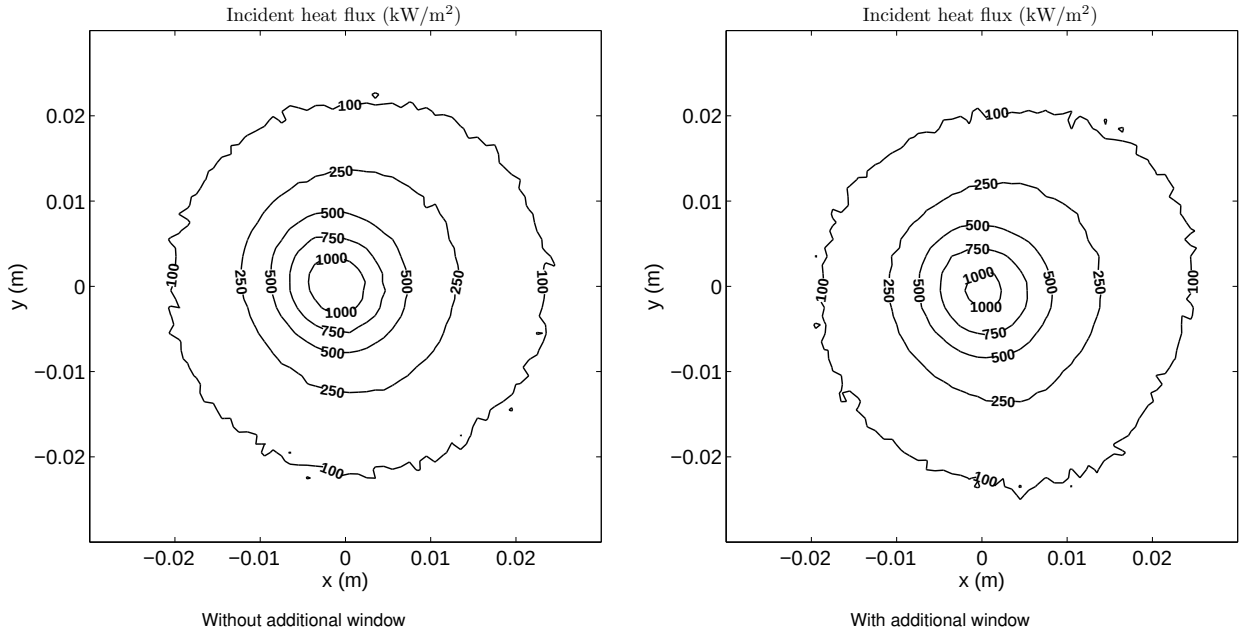

Fig. 2. Heat flux map at the focal spot

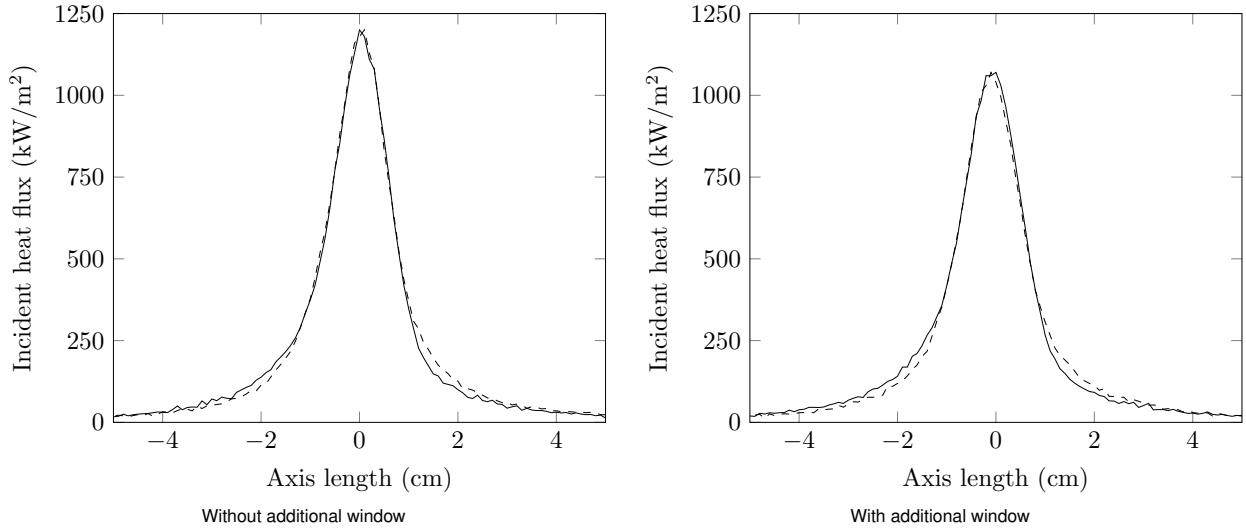

Fig. 3. Heat flux distributions at the focal spot

actor window. The window was set 5 cm above the screen, parallel to it and perpendicular to the system revolution axis. The repeatability of the measured heat flux distributions was assessed by repeating the measurement twice in both configurations. The repeatability is very good. The absorption of the window was computed with respect to the lamp radiation spectrum. The quartz window was found to absorb 7.5 % of the incident power.

3. Results

Figure 2 reports the determined heat flux distributions at the focal spot without and with the additional quartz window. The spatial distributions are similar; furthermore they both exhibit revolution symmetry. Figure 3 reports cut views of the heat flux distribution along x and y axes at the focal spot. In both configurations, the distributions along the two axes are very close. They exhibit a Gaussian shape, which is congruent with literature (7–10).

The peak heat flux was measured to be 1201 kW/m2 without the window and 1072 kW/m2 with the window (Fig. 3). The window therefore induces an 11 % decrease of the peak heat flux with respect to the unshaded configuration. Furthermore, adding a window leads the total incident power to decrease from 936 W, without the quartz sheet, to 820 W. It represent a 12 % loss of the incident power. Owing regards to the window absorption, it can be concluded that reflections induce a 4.5 % loss of the incident power.

In order to assess for the similarity in the shape of the two heat flux distributions, the heat flux distribution along x axis without the windows was multiplied by 0.88 and compared to the one measured along x axis with the window. Figure

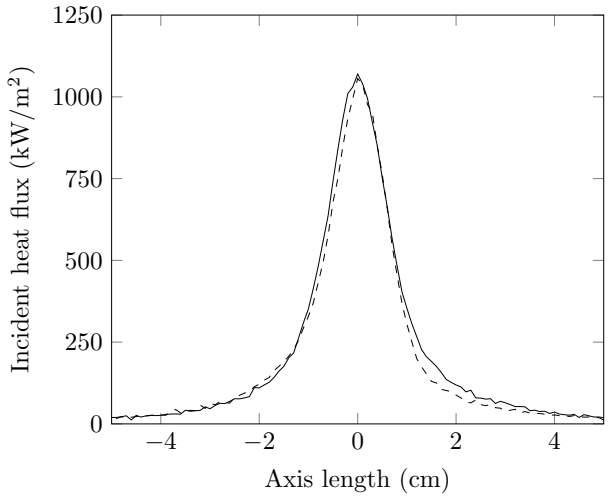

Fig. 4. Heat flux distributions at the focal spot. Continuous line: with additional window, dashed line: without additional window multiplied by 0.88

4 reports both experimentally observed and computed heat flux distributions. The two distributions are very close. It can therefore be concluded that crossing a window does not modify the shape of the heat flux distribution.

4. Conclusion

This brief note presents heat flux mappings, without and with an intermediate window, at the focal spot of a solar concentrating system. From the experimental measurements, it can be concluded that crossing a window induces a 12 % loss of the incident power and a 11 % reduction of the peak heat flux density. Furthermore, the heat flux distribution shape after crossing the window is almost identical to the one before. The two heat flux distribution shape can be linked by a simple multiplication by a 0.88 factor.

As a conclusion, it can be stated that: as a good rule of thumb, one can consider that crossing a window reduces by 12 % the total power and the peak density while conserving the shape of the heat flux distribution.

Acknowledgements

This work was funded by the French "Investments for the future" program managed by the National Agency for Research under contract ANR-10-LABX-22-01.

References

1. A. Imhof. Decomposition of limestone in a solar reactor. *Renewable Energy*, 10(2–3):239–246, 1997. ISSN 0960-1481. .
2. A. Z'Graggen and A. Steinfeld. Hydrogen production by steam-gasification of carbonaceous materials using concentrated solar energy – V. Reactor modeling, optimization, and scale-up. *International Journal of Hydrogen Energy*, 33(20):5484–5492, October 2008. ISSN 0360-3199. .
3. TP Salikhov, VV Kan, and SN Kan. Gas-phase method for obtaining nanopowders in solar furnaces. *Applied Solar Energy*, 43(1):54–55, 2007.
4. Sh A Faiziev, MS Paizullakhanov, and Sh R Nurmatov. Features of zirconium carbonitride synthesis in a large solar furnace. *Applied Solar Energy*, 46(1):53, 2010.
5. C. Guesdon, I. Alxneit, H. R. Tschudi, D. Wuillemin, J. Petrasch, Y. Brunner, L. Winkel, and M. Sturzenegger. PSI's 1 kW imaging furnace—A tool for high-temperature chemical reactivity studies. *Solar Energy*, 80(10):1344–1348, October 2006. ISSN 0038-092X. .
6. Victor Pozzobon and Sylvain Salvador. High heat flux mapping using infrared images processed by inverse methods: an application to solar concentrating systems. *Solar Energy*, 117C:29–.35, 2015. .
7. Jawad Sarwar, Grigoris Georgakis, Robert LaChance, and Nesrin Ozalp. Description and characterization of an adjustable flux solar simulator for solar thermal, thermochemical and photovoltaic applications. *Solar Energy*, 100:179–194, February 2014. ISSN 0038-092X. . WOS:000331007700018.
8. Joerg Petrasch, Patrick Coray, Anton Meier, Max Brack, Peter Haeberling, Daniel Wuillemin, and Aldo Steinfeld. A novel 50 kW 11,000 suns high-flux solar simulator based on an array of xenon arc lamps. *Journal of Solar Energy Engineering-Transactions of the Asme*, 129(4): 405–411, November 2007. ISSN 0199-6231. . WOS:000250637900008.
9. J. Llorente, J. Ballestrin, and A. J. Vazquez. A new solar concentrating system: Description, characterization and applications. *Solar Energy*, 85(5):1000–1006, May 2011. ISSN 0038-092X. . WOS:000290644000029.
10. AA Abdurakhmanov, Sh I Klychev, Sh R Nurmatov, Sh A Faiziev, and MS Paizullakhanov. Distribution of irradiance along axis of paraboloid concentrators. *Applied Solar Energy*, 45 (4):279–280, 2009.